JPET Fast Forward. Published on August 10, 2015 as DOI: 10.1124/jpet.115.225516
This article has not been copyedited and formatted. The final version may differ from this version.

JPET #225516

The impacts of spironolactone on severity of portal-systemic collaterals and hepatic encephalopathy in cirrhotic rats

Shao-Jung Hsu[1,2,3], Sun-Sang Wang[1,6], Teh-Ia Huo[2,3] Fa-Yauh Lee[1,3*], Hui-Chun Huang[1,3*], Ching-Chih Chang[1,4], I-Fang Hsin[1,2,5], Hsin-Ling Ho[3], Han-Chieh Lin[1,3], Shou-Dong Lee[1,7]

[1]Faculty of Medicine and [2]Institute of Pharmacology, National Yang-Ming University School of Medicine, [3]Division of Gastroenterology and [4]General Medicine, Department of Medicine, [5]Endoscopy Center for Diagnosis and Treatment, and [6]Department of Medical Affair and Planning, Taipei Veterans General Hospital, and [7]Division of Gastroenterology, Department of Medicine, and Cheng Hsin General Hospital, Taipei, Taiwan.

Running title: Spironolactone ameliorated portal-systemic collaterals

***Correspondence:**

Fa-Yauh Lee and Hui-Chun Huang, M.D.

Division of Gastroenterology, Department of Medicine, Taipei Veterans General Hospital

No.201, Sec.2, Shih-Pai Road, Taipei, 11217, Taiwan

TEL: +886-2-28712121 ext. 2049; FAX: +886-2-28739318

Email: fylee@vghtpe.gov.tw and hchuang2@vghtpe.gov.tw

Text pages: 18

Tables: 2

Figures: 5

References: 29

Words in the abstract: 187

Words in the introduction: 313

Words in the discussion: 1301

JPET Fast Forward. Published on August 10, 2015 as DOI: 10.1124/jpet.115.225516
This article has not been copyedited and formatted. The final version may differ from this version.

Abbreviations:

BDL, bile duct ligation; COX, cyclooxygenases; DW, distilled water; eNOS, endothelial NO synthases; H&E, hematoxylin-eosin; HR, heart rate; iNOS, inducible NO synthases; MAP, mean arterial pressure; NO, nitric oxide; PP, portal pressure; VEGF, vascular endothelial growth factor;

Recommended section assignment:

Gastrointestinal, Hepatic, Pulmonary, and Renal

JPET Fast Forward. Published on August 10, 2015 as DOI: 10.1124/jpet.115.225516
This article has not been copyedited and formatted. The final version may differ from this version.

Abstract

Liver cirrhosis and portal hypertension are accompanied by portal-systemic collaterals formation and lethal complications. Angiogenesis participates in the development of collaterals. Spironolactone is an aldosterone receptor antagonist used to control fluid overload in cirrhotic patients, although recent studies suggest that it also inhibits angiogenesis. This study aimed to investigate the effect of spironolactone on abnormal angiogenesis and portal-systemic collaterals in cirrhosis. Liver cirrhosis was induced in Spraque-Dawley rats by common bile duct ligation (BDL), while the sham-operated rats were the controls. The BDL and sham rats received spironolactone (20 mg/kg/day, oral gavage) or vehicle from the 15^{th} to 28^{th} day after the operations. Spironolactone did not influence the portal and systemic hemodynamics and the renal and hepatic biochemistry data, but significantly ameliorated hepatic fibrosis, portal-systemic shunting, and mesenteric angiogenesis. Plasma VEGF level and the mesenteric protein expressions of VEGF and phosphor-VEGFR2 decreased in the spironolactone group. Spironolactone did not affect motor activity and plasma ammonia level, either. The down-regulation of VEGF pathway participates, albeit partly, in the anti-angiogenic effect of spironolactone. Thus, spironolactone treatment in patients with liver cirrhosis may provide additional benefits aside from ascites control.

Introduction

During the progression of liver cirrhosis, portal hypertension develops due to increased splanchnic inflow and hepatic resistance. The formation of portal-systemic collaterals may divert the stagnant blood flow in the portal system. However, the shunting itself has detrimental complications like esophageal variceal bleeding and hepatic encephalopathy. Accumulating evidence demonstrates that angiogenesis, the formation of new vessels from a pre-existing vasculature, plays a pivotal role in the development and maintenance of portal hypertension (Ferneandez, et al., 2004). In addition, amelioration of splanchnic angiogenesis effectively ameliorates portal-systemic shunting (Huang, et al., 2012; Hsu, et al., 2014).

The renin-angiotensin-aldosterone system activation is a compensatory response to arterial vasodilation and “inadequate” intravascular volume associated with cirrhosis. Aldosterone is a mineralocorticoid that mediates salt and water reabsorption in the distal tubules of the kidney. Spironolactone, a potent aldosterone blocker, is thus frequently prescribed for cirrhotic patients to control fluid overload and ascites. A previous study has indicated that spironolactone significantly alleviates sodium retention when renal failure is not yet present (Wilkinson, et al., 1979). But beyond the sodium and fluid status homeostasis, aldosterone may also participate in angiogenesis. Another study indicates that aldosterone mediates the actions of

mineralocorticoid receptors in the pathologic angiogenesis of the retina and this is attenuated by spironolactone (Wilkinson-Berka, et al., 2009). Spironolactone induced a dose-dependent reduction of capillary tube formation. The fibrin gel chamber study performed in rats also demonstrated that spironolactone significantly reduces the numbers of both peripheral and central neovessels (Miternique-Grosse, et al., 2006). Spironolactone reduces neovascularization and varicocele-induced angiogenesis in rats (Köse, et al., 2012).

Since the renin-angiotensin-aldosterone system is activated in liver cirrhosis with portal hypertension, the potential of aldosterone receptor antagonist to alleviate angiogenesis has been noted. However, since its relevant influences on portal-systemic collaterals in cirrhosis have not been surveyed, this study aimed to elucidate the aforementioned aspects in rats with bile duct ligation (BDL)-induced liver cirrhosis.

Material and Methods

Animal model

Male Sprague-Dawley rats weighing 240-270 g at the time of surgery were used for experiments. Secondary biliary cirrhosis was induced by common bile duct ligation as previously described (Huang, et al., 2012; Hsu, et al., 2014). Under ketamine anesthesia (100 mg/kg, intramuscularly), the common bile duct was exposed through a midline abdominal incision, catheterized by a PE-10 catheter, and doubly ligated with 3-0 silk. The first ligature was made below the junction of the hepatic ducts and the second ligature above the entrance of the pancreatic duct followed by section of the common bile duct between the ligatures. The rats were allowed to recover. A high yield of secondary biliary cirrhosis was noted four weeks after the ligation. To avoid the coagulation defects, BDL rats received weekly vitamin K injection (50 μg/kg intramuscularly).

The Taipei Veterans General Hospital Animal Committee approved the study (Grant number IACUC 2013-095). All animals received humane care according to the criteria outlined in the "Guide for the Care and Use of Laboratory Animals" prepared by the National Academy of Sciences and published by the National Institutes of Health (NIH publication 86-23 revised 1985).

JPET Fast Forward. Published on August 10, 2015 as DOI: 10.1124/jpet.115.225516
This article has not been copyedited and formatted. The final version may differ from this version.

Therapeutic effects of spironolactone on BDL rats

The BDL and sham rats received spironolactone (20 mg/kg/day, oral gavage) or vehicle from the 15th to the 28th day post-operatively.

Measurement of systemic and portal hemodynamics

The right femoral artery was cannulated with a PE-50 catheter connected to a Spectramed DTX transducer (Spectramed Inc., Oxnard, CA). Continuous recordings of mean arterial pressure (MAP), heart rate (HR), and portal pressure (PP) were performed on a multi-channel recorder (model RS 3400, Gould Inc., Cupertino, CA). The external zero reference was placed at the level of the mid-portion of the rat. The abdomen was then opened with a mid-line incision, and a mesenteric vein was cannulated with a PE-50 catheter connected to a Spectramed DTX transducer. The abdominal cavity was closed and the portal pressure was recorded.

Hepatic fibrosis determination with Sirius red staining

A liver paraffin section was stained with a Sirius red staining kit (Polysciences Inc., Warrington, PA). Image J was used to measure the percentage of Sirius red-stained area. Briefly, grayscale image was used, then the red-stained collagen was

JPET Fast Forward. Published on August 10, 2015 as DOI: 10.1124/jpet.115.225516
This article has not been copyedited and formatted. The final version may differ from this version.

isolated using thresholding function. After that, the thresholded area was measured and shown as the percentage of threshold area per image.

Immunofluorescent study for liver macrophage

Liver macrophage and Kupffer cells were evaluated by CD68 staining. In brief, the liver paraffin sections were dewaxed and retrieved with heat citrate buffer. The sections were then incubated with monoclonal anti-CD68 [1:100; AbD Serotec, Oxford, UK] for 1 hour, followed by fluorescent conjugated 2nd antibody. Macrophage and Kupffer cell amount were determined by thresholding the X200 images using Image J software. Four areas from each sample were quantified.

Hematoxylin and Eosin Staining

Tissue was fixed in 10% formalin, embedded in paraffin, sectioned in 5 μm, and stained with hematoxylin-eosin (H&E).

Color microsphere method for portal-systemic shunting degree analysis

Portal-systemic shunting degree was determined using the technique described by Chojkier and Groszmann and substituted color for radioactive microspheres;

30,000 of 15-μm yellow microspheres (Dye Track; Triton Technology, San Diego, CA)(Chojkier and Groszmann, 1981). Portal-systemic shunting was calculated as lung microspheres/(liver microspheres lung microspheres). Assuming a worst-case scenario in which two-thirds of the microspheres remain trapped in the spleen, this technique detected a minimum shunt of 3.5%. Studies using color microspheres have been shown to provide results similar to those using radioactive microspheres (Hodeige, et al., 1999).

Immunofluorescent study for mesenteric vascular density

Splanchnic angiogenesis was evaluated by assessing the CD31-labeled microvascular networks in rat mesenteric connective tissue windows, which was performed as previously described (Huang, et al., 2012; Hsu, et al., 2014). (×100)-magnification immunofluorescent images were assessed using an upright fluorescent microscope (AX80, Olympus, Japan) and thresholded by Image J software. Vascular length was manually measured with the pencil tool and the vascular area automatically with histogram function, respectively. The unit of vascular length per unit area of mesenteric window would be $\mu m/\mu m^2 = \mu m^{-1}$ and the vascular area per unit area of mesenteric window, actually, could be pixel/pixel without being converted to $\mu m^2/\mu m^2$.

Plasma vascular endothelial growth factor (VEGF) determination

Plasma VEGF levels were measured using an enzyme-linked immunoabsorbent assay kits (R&D Systems Inc., MN) according to the manufacturer's instructions. The intensity of the color was measured at the absorbance of 450–600 nm with a Bio-kinetics Reader (Bio-Tek Instruments Inc., VT). The intra- and interassay variations of these assays were less than 10%.

Western analysis

Protein expression was analyzed by western blotting as previously described.[2,3] Blots were incubated with the primary antibody [inducible NO synthases (iNOS), endothelial NO synthases (eNOS), cyclooxygenases-1 (COX-1), and cyclooxygenases-2 (COX-2): Cell Signaling Technology, Beverly, MA; VEGF, phospho-VEGFR-2: Santa Cruz Biotechnology, Santa Cruz, CA].

Motor activities

Motor activities in an open field were determined by an opto-Varimex animal activity meter (Columbus Instruments Inc.) as previously stated (Hsu, et al., 2012). The Opto-Varmex activity sensors utilized high-intensity, modulated infrared light beams to detect animal motion. Animals were housed in transparent cages (17 x 17 x 8 inches; 43 x 43 x 20 cm) through which 30 infrared beams passed in the horizontal

JPET Fast Forward. Published on August 10, 2015 as DOI: 10.1124/jpet.115.225516
This article has not been copyedited and formatted. The final version may differ from this version.

plane, 15 on each axis. This device differentiated nonambulatory movements (scratching, gnawing) from ambulation on the basis of consecutive interruption of the infrared monitoring beams. An additional row of infrared beams in the horizontal plane (15 on each axis) about 10 cm above the floor was used to count the vertical movements. During the activity measurements, animals had no access to food or chow. All studies were performed under strictly standardized conditions in the dark room for 30 minutes. The total, ambulatory, and vertical movements were recorded to reflect the motor activities of the rats.

Drugs

Except for those already cited in the text, spironolactone was purchased from Sigma Chemical Co. (St. Louis, MO).

Data analysis

All results are expressed as mean ± S.E.M. Statistical analyses were performed using an independent Student's *t*-test or ANOVA with Tukey's test as appropriate. Results were considered statistically significant at a two-tailed *P*-value less than 0.05.

JPET Fast Forward. Published on August 10, 2015 as DOI: 10.1124/jpet.115.225516
This article has not been copyedited and formatted. The final version may differ from this version.

Results

Body weight and hemodynamics

The hemodynamic results of the sham or BDL-operated rats treated with either DW or spironolactone were shown in Table 1. Compared with sham rats, BDL rats had significantly lower body weight (BW), lower MAP, and higher PP, which was not significantly modified by spironolactone.

Plasma liver and kidney biochemistry parameters

Table 2 depicts the liver and kidney biochemistry parameters of experimental groups. There was no significant difference between spironolactone- and paralleled DW-treated groups.

Liver fibrosis

Figure 1(A) reveals Sirius red stained fibrotic area ratio in the liver. Spironolactone significantly attenuated liver fibrosis in cirrhotic rats (BDL-DW vs. BDL-spironolactone (%): 16.1±0.5 vs. 12.2±0.5; $P < 0.001$).

Liver macrophage

JPET Fast Forward. Published on August 10, 2015 as DOI: 10.1124/jpet.115.225516
This article has not been copyedited and formatted. The final version may differ from this version.

Figure 1(B) discloses CD68 staining area ratio in the periportal area of the liver. Compared to DW-treated control group, spironolactone significantly decreased macrophage content in the periportal area of cirrhotic livers (BDL-DW vs. BDL-spironolactone (%): 1.04±0.10 vs. 0.51±0.05; $P = 0.036$).

Portal-systemic shunting

Figure 2 depicts the severity of portal-systemic shunting in all groups. Compared with vehicle, cirrhotic (BDL) rats treated with spironolactone had significantly less shunting (BDL-DW vs. BDL-spironolactone: shunting degree (%): 77.5±2.6 vs. 33.4±6.6 ; $P < 0.001$).

Mesenteric vascular density

The parameters of mesenteric vascular density are shown in figure 3 (A). In BDL groups, spironolactone significantly decreased the vascular length and vascular area (BDL-DW vs. BDL-spironolactone: vascular length per unit window area (μm^{-1}): 0.0182±0.0009 vs. 0.0111±0.0007; $P < 0.001$; vascular area per unit window area (%): 12.91±0.77 vs. 7.79±0.58; $P < 0.001$).

Plasma VEGF determination

JPET Fast Forward. Published on August 10, 2015 as DOI: 10.1124/jpet.115.225516
This article has not been copyedited and formatted. The final version may differ from this version.

Figure 4(A) depicts the levels of plasma VEGF. Spironolactone significantly reduced the plasma VEGF level in BDL rats (BDL-DW vs. BDL-spironolactone: 25.8±1.1 vs. 19.7±1.8 ρg/ml; $P = 0.007$).

Mesenteric angiogenic proteins expressions

The expressions of mesenteric angiogenic proteins are shown in figure 4(B). The protein main angiogenic factor, VEGF, and activation of its target receptor, phospho-VEGFR-2 were down-regulated significantly in spironolactone-treated BDL rats compared to DW-treated BDL rats (BDL-DW vs. BDL-spironolactone: VEGF: 0.92±0.69 vs. 0.42±0.03; $P = 0.014$; phospho-VEGFR-2: 1.75±0.15 vs. 1.11±0.15; $P = 0.029$). There was no significant difference in iNOS, eNOS, COX-1, and COX-2, protein expressions between the two groups.

Motor activities and plasma ammonia concentration

Figure 5(A) shows the motor activity of all groups. Comported with sham-operated group, rats received BDL operation had lower motor activities. Consistently, the plasma ammonia concentration increased in BDL rats (figure 5(B)). On the other hand, spironolactone treatment in BDL rats exerted no significant effect on motor activities and plasma ammonia concentration.

Discussion

Common bile duct ligation (BDL) is a well-established animal model widely applied to evaluate the pharmacologic aspects of chronic liver injury. It also reflects pathophysiologic change of renin-angiotensin-aldosterone axis during the progression of liver cirrhosis (Jonassen, et al., 1998; Kim, et al., 2006). In terms of pharmacological studies, prophylactic and therapeutic strategies can be designed with this model, depending on the timing of treatments (Hsu, et al., 2015). Because liver fibrosis usually develops on the 14^{th} day and liver cirrhosis is established on the 28^{th} day after BDL (Kountouras, et al., 1984), therapeutic agents administered immediately after BDL is usually regarded as the prophylactic strategy. On the other hand, agents given since fibrosis formation may serve as the therapeutic strategy, which is more relevant to the clinical condition, whereby patients suffering from chronic liver diseases-related symptoms and complications seek help then receive treatments.

In this study, spironolactone treatment with therapeutic strategy in cirrhotic rats significantly ameliorated hepatic fibrosis, portal-systemic collateral shunting and mesenteric angiogenesis, but PP was not influenced. A recent survey indicated that spironolactone treatment with prophylactic strategy alleviated liver fibrosis and

reduced PP (Luo, et al., 2012). Another study showed that prophylactic spironolactone treatment significantly decreased PP and portal-systemic shunts (Oberti, et al., 1997). Such different influences of spironolactone on PP suggest that the portal hypotensive effect can be exerted by early spironolactone treatment at the start of liver injury. However, the use of spironolactone at the very beginning of hepatic damage is not prevalent in the clinical setting. In this study, even though spironolactone treatment started since the development of liver fibrosis failed to modify PP, it still significantly attenuated liver fibrosis and portal-systemic collaterals in BDL rats. Taken together, spironolactone treatment with a “therapeutic” but not “prophylactic” strategy is beneficial and clinically relevant but the appropriate regimen for patients requires further investigation.

Angiogenesis plays a pivotal role in the formation of portal-systemic collaterals in portal hypertension (Fernandez, et al., 2004). Regarding the potential influence of aldosterone on angiogenesis, a human study found that tumor vascularization was positively associated with aldosterone (Bernini, et al., 2002). Aldosterone also enhanced ischemia-induced neovascularization (Michel, et al., 2004). Consistently, spironolactone treatment in this study ameliorated abnormal splanchnic angiogenesis in cirrhosis. Spironolactone is also a testosterone antagonist and the previous study had identified that spironolactone attenuated neovascularization through inhibition of

VEGF pathway (Klauber, et al., 1996). However, cyproterone, another testosterone antagonist, was not effective in anti-angiogenesis. Furthermore, although spironolactone had anti-mineralocorticoid effects, it suppressed neovascularization in aldosterone-free culture media. Taken together, the anti-angiogenesis activity of spironolactone could be unrelated to its antiandrogenic and antimineralocorticoid effects (Gökhan-Köse, et al., 2014; Klauber, et al., 1996).

Among the possibly implicated angiogenic factors, VEGF is a potent mitogen that stimulates endothelial proliferation and differentiation, acting mainly via its binding to VEGFR-2 (Terman, et al., 1992). Inhibition of the VEGF signaling pathway has been proved to reverse portal hypertension-related pathological angiogenesis (Fernandez, et al., 2005). Aldosterone-producing adrenal adenomas expressed higher levels of VEGF (Bernini, et al., 2002). Aldosterone also increased VEGF protein expression in a mice model with ischemia (Michel, et al., 2004). Moreover, spironolactone inhibited both basic fibroblast growth factor (bFGF)- and VEGF-stimulated endothelial cell proliferation and capillary endothelial cell chemotaxis toward bFGF *in vitro* (Klauber, et al., 1996). In this study, spironolactone significantly decreased both plasma VEGF level and mesenteric VEGF protein expression. Furthermore, the phosphorylation of its target receptor, VEGFR-2, diminished at the same time. This finding suggests that spironolactone attenuated

JPET Fast Forward. Published on August 10, 2015 as DOI: 10.1124/jpet.115.225516
This article has not been copyedited and formatted. The final version may differ from this version.

splanchnic and collateral angiogenesis by down regulating the VEGF pathway.

Although the potential detrimental effects of dampening VEGF pathway are not to be overlooked, it can be clinically feasible due to the following reasons: First, sorafenib, a multikinase inhibitor that inhibits angiogenesis via VEGF pathway blockade, is nowadays a recommended target therapy for hepatocellular carcinoma, which is usually developed in cirrhotic patients. Until now, there are no remarkable adverse effects related to anti-angiogenesis reported. Second, clinical experiences of spironolactone for patients with cirrhosis or heart failure indicate that the major side effects of spironolactone are hyperkalemia, gynecomastia, and pre-renal azotemia, in which none of them is attributable to anti-angiogenesis. Third, in the current study, the mesenteric vascular density of the spironolactone-treated sham rats was not significantly different from that of the vehicle-treated sham rats, suggesting that spironolactone did not affect the relatively normal vasculature. As a result, we think aldosterone application in cirrhosis is considerably safe in terms of its anti-angiogenesis effect.

Prostacyclin and nitric oxide (NO) are synthesized by cyclooxygenases (COX-1 and COX-2) and NO synthases (eNOS and iNOS), respectively, and participate in the hyperdynamic circulation and vascular derangement in portal hypertension. They are, in fact, also angiogenic factors (Gupta, et al., 2003; Klenke, et al., 2006; Sumanovski,

et al., 1999). Regarding the inter-relationship between mineralocorticoid and NO or prostaglandins, study demonstrated that down regulated expression of eNOS protein in the aorta of failing rats with myocardial ischemia can be restored with eplerenone administration (Schäfer, et al., 2003). Aldosterone has also been found to increase the COX-2 expression in bovine retinal endothelial cells and retinal pericytes (Wilkinson-Berka, et al., 2009). Nevertheless, in this study, spironolactone does not affect the mesenteric protein expressions of COX-1, COX-2, iNOS and eNOS. The various results may be related to different animal models and experimental settings.

The antifibrotic and the anti-angiogenic effects may be mediated by different mechanisms. In heart, several studies suggested that mineralocorticoid antagonists prevented cardiac fibrosis by inhibiting inflammatory cells infiltration. In cirrhosis, spironolactone ameliorated hepatic fibrosis by inhibiting hepatic stellate cells activation through mineralocorticoid-TGF-β pathway (Luo, et al., 2012; Wang, et al., 2014). It is interesting that inflammatory cytokine decreased at the same time (Luo, et al., 2012). Furthermore, eplerenone, a selective mineralocorticoid antagonist, attenuated inflammatory cell infiltration in mice with steatohepatitis (Wada, et al., 2013). In this study, spironolactone significantly attenuated hepatic fibrosis and macrophage amount. This is consistent with the previous studies, suggesting that spironolactone ameliorated hepatic fibrosis at least partly through suppressing

JPET Fast Forward. Published on August 10, 2015 as DOI: 10.1124/jpet.115.225516
This article has not been copyedited and formatted. The final version may differ from this version.

macrophage infiltration.

The finding that PP is not affected by spironolactone also reflects the complicated interplay of hemodynamic factors in liver cirrhosis. Portal hypertension is determined by three major factors: augmented hepatic resistance, increased splanchnic inflow, and portal-systemic collaterals (Hsu and Huang, 2013). Among them, the collateral vascular bed is a double-edged sword. The shunting vessels release stagnant blood in portal system. However, they are responsible for lethal complications such as esophageal variceal bleeding and hepatic encephalopathy. In this study, spironolactone decreased hepatic fibrosis and mesenteric angiogenesis, which reduced the hepatic resistance and portal inflow and potentially reduced PP. However, this might have been offset by the decreased portal-systemic collaterals found in this study, which reduced the diversion of portal blood flow.

Although spironolactone ameliorated portal-systemic collaterals in the present study, the ammonia level and motor activities were not influenced, suggesting that the severity of hepatic encephalopathy was not alleviated along with diminished collaterals. In addition, the liver biochemistry data were not modified by spironolactone. Hepatic encephalopathy is driven by two major factors: the escape of ammonia and noxious substances from collaterals to central venous system and the failure of compromised hepatocytes to manage ammonia via the urea cycle. In line

with this finding, we have identified previously that in BDL rats, serum total bilirubin levels, but not the severity of collaterals, was significantly and negatively correlated with the motor activity counts. That is, the portal-systemic shunting plays a minor role than liver function in the development of hepatic encephalopathy (Hsin, et al., 2012).

In conclusion, spironolactone treatment initiated at the onset of hepatic fibrosis can significantly attenuate fibrosis progression, portal-systemic collateral shunting and mesenteric angiogenesis. The antiangiogenic effect of spironolactone is accompanied by VEGF pathway down-regulation. Spironolactone does not influence liver biochemistry and hepatic encephalopathy. Spironolactone treatment in cirrhotic patients may exert additional benefits other than ascites control.

Authorship Contributions

Participated in research design: Wang, Huo, Chang, Hsin, Ho, Lin and S.D Lee

Conducted experiments: Hsu and Huang

Performed data analysis: Hsu and Huang

Wrote or contributed to the writing of the manuscript: Hsu, F.Y. Lee and Huang

References

Bernini GP, Moretti A, Bonadio AG, Menicagli M, Viacava P, Naccarato AG, Iacconi P, Miccoli P and Salvetti A (2002) Angiogenesis in human normal and pathologic adrenal cortex. *J Clin Endocrinol Metab* **87**: 4961-4965.

Chojkier M and Groszmann RJ (1981) Measurement of portal-systemic shunting in the rat by using γ-labeled microspheres. *Am J Physiol* **240**: G371–375.

Fernandez M, Vizzutti F, Garcia-Pagan JC, Rodes J and Bosch J (2004) Anti-VEGF receptor-2 monoclonal antibody prevents portal-systemic collateral vessel formation in portal hypertensive mice. *Gastroenterology* **126**: 886-894.

Fernandez M, Mejias M, Angermayr B, Garcia-Pagan JC, Rodes J and Bosch J (2005) Inhibition of VEGF receptor-2 decreases the development of hyperdynamic splanchnic circulation and portal-systemic collateral vessels in portal hypertensive rats. *J Hepatol* **43**: 98-103.

Gökhan-Köse M, Erdem ŞR, Peşkircioğlu ÇL and Çaylak B (2014) Angiogenesis

inhibition impairs testicular morphology in experimental left varicocele rat model. *Actas Urol Esp* **38**:459-464.

Gupta RA, Tejada LV, Tong BJ, Das SK, Morrow JD, Dey SK and DuBois RN (2003) Cyclooxygenase-1 is overexpressed and promotes angiogenic growth factor production in ovarian cancer. *Cancer Res* **63**: 906-911.

Hodeige D, de Pauw M, Eechaute W, Weyne J and Heyndrickx GR (1999) On the validity of blood flow measurement using colored microspheres. *Am J Physiol* **276**: H1150-1158.

Hsin IF, Wang SS, Huang HC, Lee FY, Chan CY, Chang CC, Hsu CY, Lin HC and Lee SD (2012) Portosystemic collaterals are not prerequisites for the development of hepatic encephalopathy in cirrhotic rats. *J Chin Med Assoc* **75**: 3-9.

Hsu SJ, Hsin IF, Lin YL, Chen YC, Huang HC, Lee FY, Lin HC, Chang CC and Lee SD (2012) The influence of sorafenib on hepatic encephalopathy and the mechanistic survey in cirrhotic rats. *Eur J Clin Invest* **42**: 1309-1316.

Hsu SJ and Huang HC (2013) Management of ascites in patients with liver cirrhosis: recent evidence and controversies. *J Chin Med Assoc* **76**: 123-30.

Hsu SJ, Lee FY, Wang SS, Hsin IF, Lin TY, Huang HC, Chang CC, Chuang CL, Ho HL, Lin HC and Lee SD (2015) Caffeine ameliorates hemodynamic derangements and portosystemic collaterals in cirrhotic rats. *Hepatology* **61**: 1672-1684.

Huang HC, Wang SS, Hsin IF, Chang CC, Lee FY, Lin HC, Chuang CL, Lee JY, Hsieh HG and Lee SD (2012) Cannabinoid receptor 2 agonist ameliorates mesenteric angiogenesis and portosystemic collaterals in cirrhotic rats. *Hepatology* **56**: 248-258.

Jonassen TE, Petersen JS, Sørensen AM, Andreasen F and Christensen S (1998) Aldosterone receptor blockade inhibits increased furosemide-sensitive sodium reabsorption in rats with liver cirrhosis. *J Pharmacol Exp Ther* **287**:931-936.

Kim SW, Wang W, Sassen MC, Choi KC, Han JS, Knepper MA, Jonassen TE, Frøkiaer J and Nielsen S (2006) Biphasic changes of epithelial sodium channel abundance and trafficking in common bile duct ligation-induced liver cirrhosis. *Kidney Int* **69**:89-98.

Klauber N, Browne F, Anand-Apte B and D'Amato RJ (1996) New activity of spironolactone. Inhibition of angiogenesis in vitro and in vivo. *Circulation* **94**: 2566-2571.

Köse MG, Erdem ŞR, Pe□kircioğlu ÇL and Çaylak B (2012) Effects of angiogenesis inhibition by spironolactone on isolated vas deferens contractility in an experimental varicocele model in rats. *Urology* **80**: 816-821.

Klenke FM, Gebhard MM, Ewerbeck V, Abdollahi A, Huber PE and Sckell A (2006) The selective Cox-2 inhibitor celecoxib suppresses angiogenesis and growth of secondary bone tumors: an intravital microscopy study in mice. *BMC Cancer* **6**: 9.

Kountouras J, Billing BH and Scheuer PJ (1984) Prolonged bile duct obstruction: a new experimental model for cirrhosis in the rat. *Br J Exp Pathol* **65**: 305-311.

Luo W, Meng Y, Ji HL, Pan CQ, Huang S, Yu CH, Xiao LM, Cui K, Ni SY, Zhang ZS and Li X (2012) Spironolactone lowers portal hypertension by inhibiting liver fibrosis, ROCK-2 activity and activating NO/PKG pathway in the bile-duct-ligated rat. *PLoS*

One **7**: e34230.

Michel F, Ambroisine ML, Duriez M, Delcayre C, Levy BI and Silvestre JS (2004) Aldosterone enhances ischemia-induced neovascularization through angiotensin II-dependent pathway. *Circulation* **109**: 1933-1937.

Miternique-Grosse A, Griffon C, Siegel L, Neuville A, Weltin D and Stephan D (2006) Antiangiogenic effects of spironolactone and other potassium-sparing diuretics in humnan umbilical vein endothelial cells and in fibrin gel chambers implanted in rats. J *Hypertens* **24**: 2207-13.

Oberti F, Pilette C, Rifflet H, Maïga MY, Moreau A, Gallois Y, Girault A, le Bouil A, Le Jeune JJ, Saumet JL, Feldmann G and Calès P (1997) Effects of simvastatin, pentoxifylline and spironolactone on hepatic fibrosis and portal hypertension in rats with bile duct ligation. *J Hepatol* **26**: 1363-1371.

Schäfer A, Fraccarollo D, Hildemann SK, Tas P, Ertl G and Bauersachs J (2003) Addition of the selective aldosterone receptor antagonist eplerenone to ACE inhibition in heart failure: effect on endothelial dysfunction. *Cardiovasc Res* **58**: 655-662.

Sumanovski LT, Battegay E, Stumm M, Van Der Kooij M and Sieber CC (1999) Increased angiogenesis in portal hypertensive rats: role of nitric oxide. *Hepatology* **29**: 1044-1049.

Terman BI, Dougher-Vermazen M, Carrion ME, Dimitrov D, Armellino DC, Gospodarowicz D and Böhlen P (1992) Identification of the KDR tyrosine kinase as a receptor for vascular endothelial cell growth factor. *Biochem Biophys Res Commun* **187**: 1579-1586.

Wada T, Miyashita Y, Sasaki M, Aruga Y, Nakamura Y, Ishii Y, Sasahara M, Kanasaki K, Kitada M, Koya D, Shimano H, Tsuneki H and Sasaoka T (2013) Eplerenone ameliorates the phenotypes of metabolic syndrome with NASH in liver-specific SREBP-1c Tg mice fed high-fat and high-fructose diet. *Am J Physiol Endocrinol Metab* **305**:E1415-1425.

Wang S, Zhang Z, Zhu X, Wu H, Gao H and Yang C (2014) Effect of aldosterone and its antagonist on the expression of PAI-1 and TGF-β1 in rat hepatic stellate cells. *Int J Clin Exp Med* **7**:4677-4685.

Wilkinson SP, Jowett TP, Slater JDH, Arroyo V, Moodie H and Williams R (1979) Renal sodium retention in cirrhosis: relation to aldosterone and nephron site. *Clin Sci* **56**: 169-177.

Wilkinson-Berka JL, Tan G, Jaworski K and Miller AG (2009) Identification of a retinal aldosterone system and the protective effects of mineralocorticoid receptor antagonism on retinal vascular pathology. *Circ Res* **104**: 124-133.

Footnotes

Disclosures

This work was supported by Taipei Veteran General Hospital [Grant number V103C-082].

Conflicts

The authors have no conflicts of interest.

Figure legends

Figure 1. Liver histology. (A) Spironolactone significantly reduced the ratio of liver fibrosis in cirrhotic rats. (B) Spironolactone significantly decreased the amount of liver macrophages over peri-portal area in cirrhotic rats. (C) Illustrative figures. The upper and middle panels are the representative figures of Sirius red staining and H&E staining, respectively. The lower panel shows the representative figures of CD68 staining. BDL: bile duct ligation; D: distilled water; S: spironolactone. *P<0.05

Figure 2. Severity of portal-systemic shunting. Compared to the sham-D group, the BDL operation and distilled water treatment group had significantly higher portal-systemic shunting degree, significantly reduced by spironolactone. *P<0.05.

Figure 3. Mesenteric vascular density. (A) Compared to sham rats, the parameters of mesenteric vascular density significantly increased in BDL rats treated with distilled water, which were attenuated by spironolactone. (B) Representative figures of mesenteric CD31 immunofluorescence staining.

JPET Fast Forward. Published on August 10, 2015 as DOI: 10.1124/jpet.115.225516
This article has not been copyedited and formatted. The final version may differ from this version.

*P<0.05.

Figure 4. Angiogenic factors expression. (A) Spironolactone significantly reduced plasma VEGF concentration in BDL rats. (B) In the BDL rats with spironolactone treatment, the mesenteric VEGF and phospho-VEGFR-2 protein expression decreased significantly compared to distilled water-treated BDL rats. *P<0.05.

Figure 5. Motor activities and plasma ammonia concentration. (A) BDL rats had lower motor activities compared to sham rats. Spironolactone did not influence motor activity in BDL-cirrhotic rats. (B) Cirrhotic rats had higher plasma ammonia concentration. Spironolactone did not affect plasma ammonia concentration. *P<0.05.

JPET Fast Forward. Published on August 10, 2015 as DOI: 10.1124/jpet.115.225516
This article has not been copyedited and formatted. The final version may differ from this version.

Table 1. Body weight and hemodynamic parameters in sham or BDL rats with (vehicle) or spironolactone treatment

	sham-D	**sham-S**	**BDL-D**	**BDL-S**
	n=7	n=5	n=7	n=7
BW (g)	481±14	473±13	421±7*	403±11
MAP (mmHg)	113±4	104±9	90±6*	90±3
HR (beats/min)	337±31	317±22	318±17	284±17
PP (mmHg)	7.93±0.25	6.00±0.78	15.52±1.12*	15.53±1.13

S: spironolactone; D: distilled water (control); BDL: bile duct ligation; BW: body weight; MAP: mean arterial pressure; HR: heart rate; PP: portal pressure.
† *P*>0.05 between BDL-S group and BDL-D group in all parameters;
* *P*<0.05, BDL-D group vs. sham-D group.

JPET Fast Forward. Published on August 10, 2015 as DOI: 10.1124/jpet.115.225516
This article has not been copyedited and formatted. The final version may differ from this version.

Table 2. Plasma biochemistry parameters in sham or BDL rats with DW or spironolactone treatment

	sham-D	**sham-S**	**BDL-D**	**BDL-S**
	n=7	n=5	n=7	n=7
AST(U/L)	100±6	89±7	753±77*	802±115
ALT(U/L)	48±3	47±4	170±17*	190±20
BUN(mg/dl)	17.6±1.8	18.0±0.8	18.5±1.0	19.9±0.9
Creatinine(mg/dl)	0.17±0.00‡	0.20±0.03	0.17±0.00‡	0.17±0.00‡
Na	138.9±0.7	140.0±1.1	139.6±0.8	140.4±0.7
K	5.4±0.4	5.5±0.7	6.5±0.7	7.6±1.0

S: spironolactone; D: distilled water (control); BDL: bile duct ligation; AST: aspartate transaminase; ALT: alanine transaminase; BUN: blood urea nitrogen;
† $P>0.05$ between BDL-S group and BDL-D group in all parameters;
‡ Under the detection limit (0.17mg/dl)
* $P<0.05$, BDL-D group vs. sham-D group.

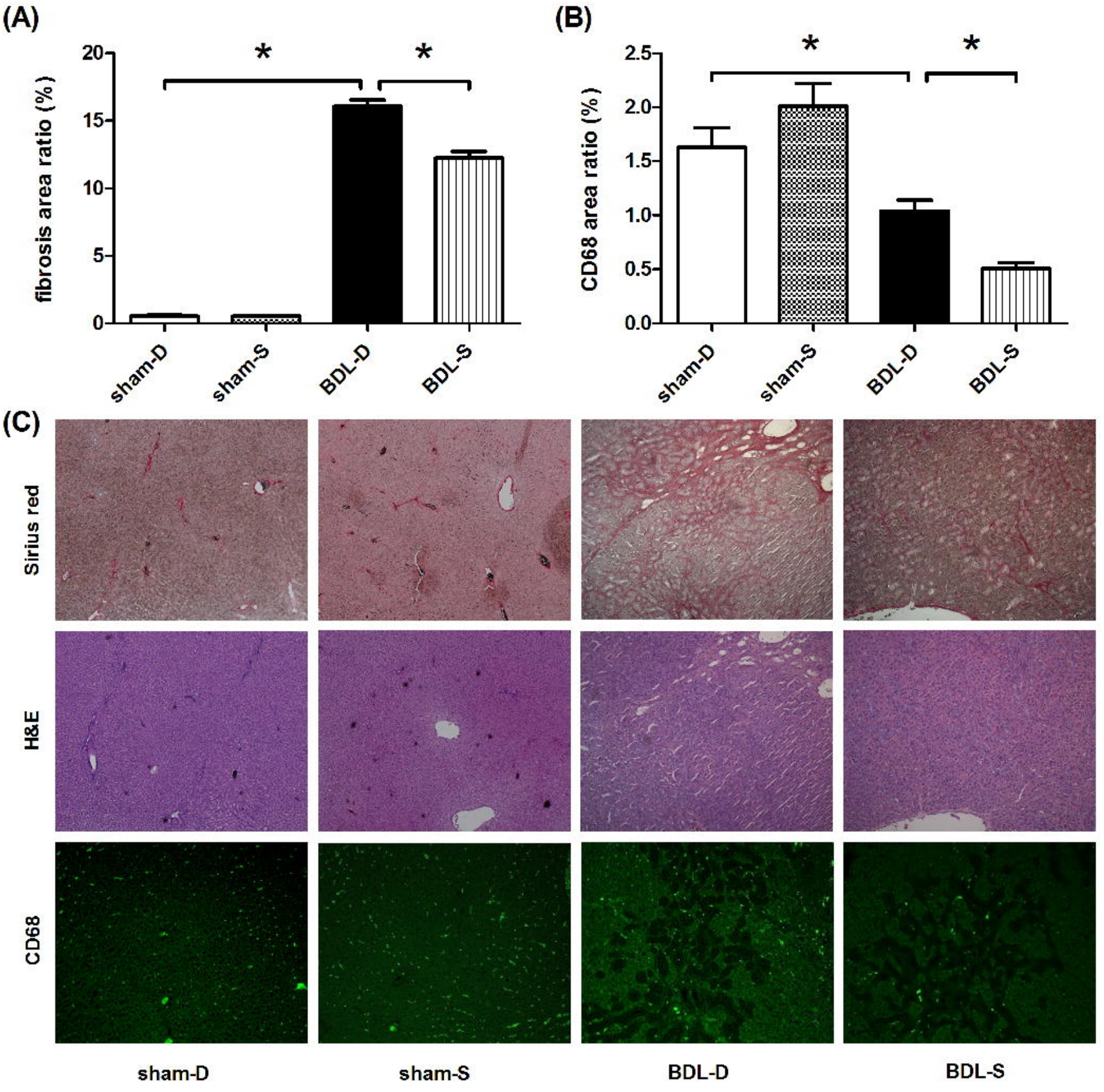
(A)
fibrosis area ratio (%)
20
15
10
5
0
*
*
sham-D
sham-S
BDL-D
BDL-S
(B)
CD68 area ratio (%)
2.5
2.0
1.5
1.0
0.5
0.0
*
*
sham-D
sham-S
BDL-D
BDL-S
(C)
Sirius red
H&E
CD68
sham-D
sham-S
BDL-D
BDL-S

Figure 1

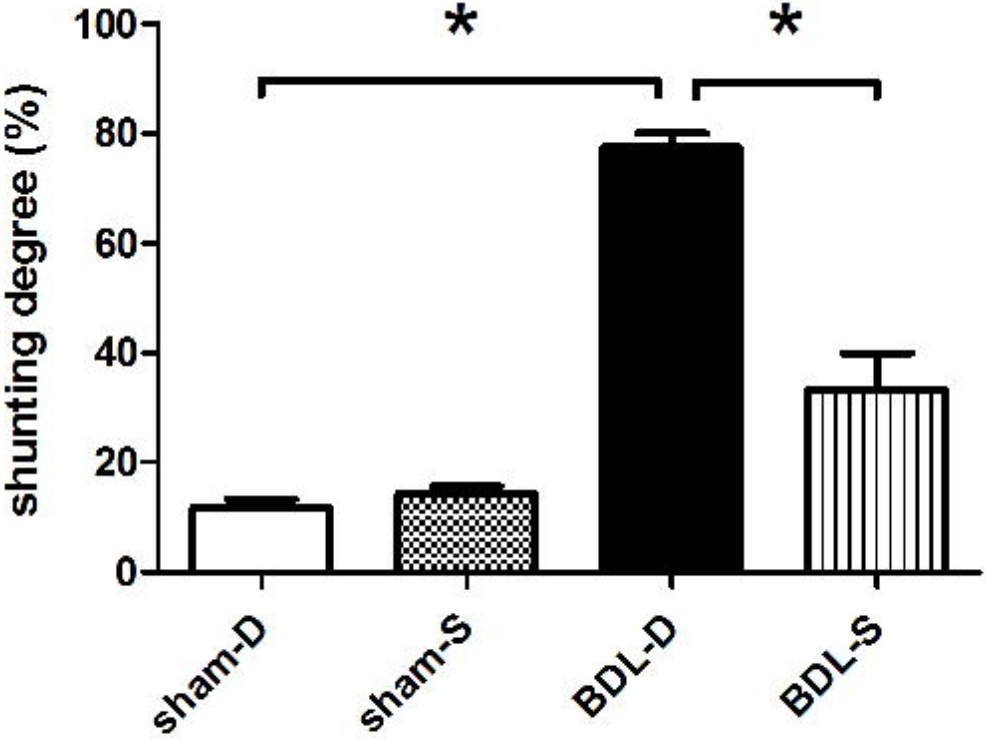

Figure 2

(A)

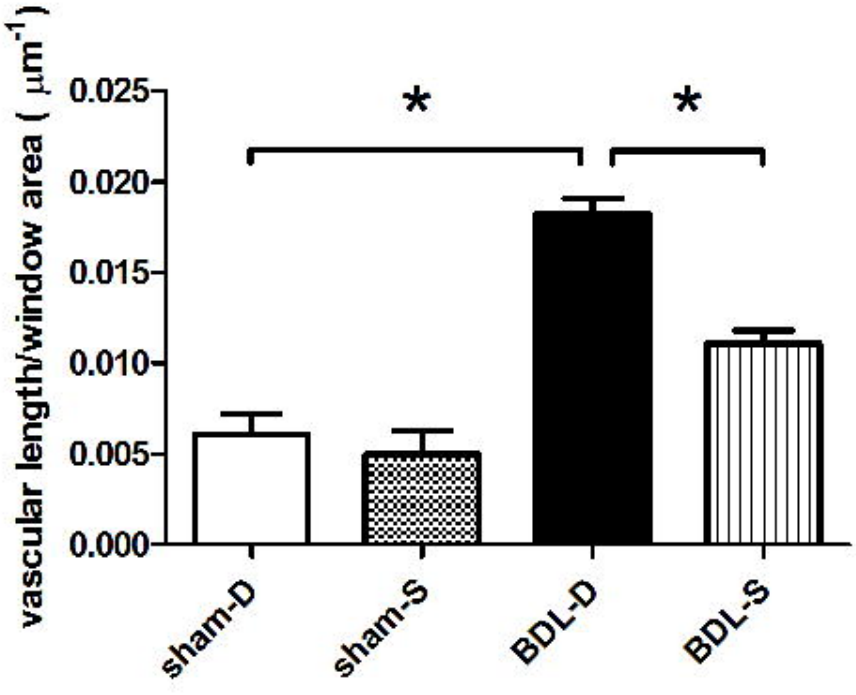
vascular length/window area (μm-1)
0.025
0.020
0.015
0.010
0.005
0.000
*
*
sham-D
sham-S
BDL-D
BDL-S

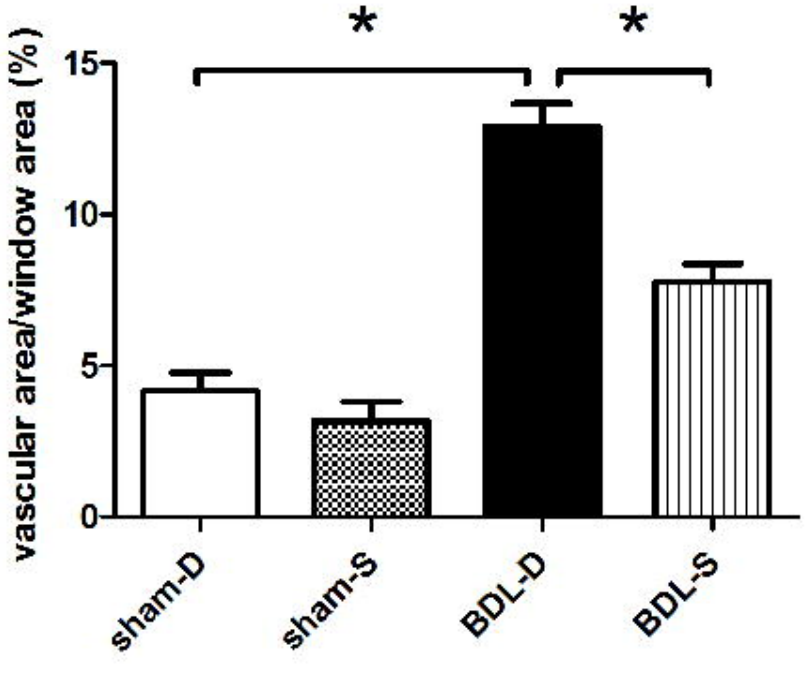
vascular area/window area (%)
15
10
5
0
*
*
sham-D
sham-S
BDL-D
BDL-S

(B)

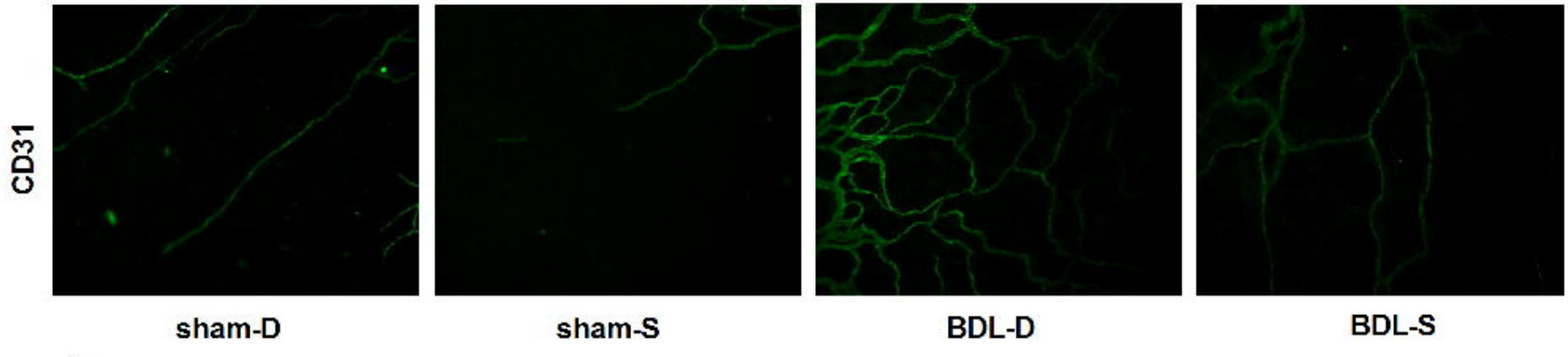
CD31
sham-D
sham-S
BDL-D
BDL-S

Figure 3

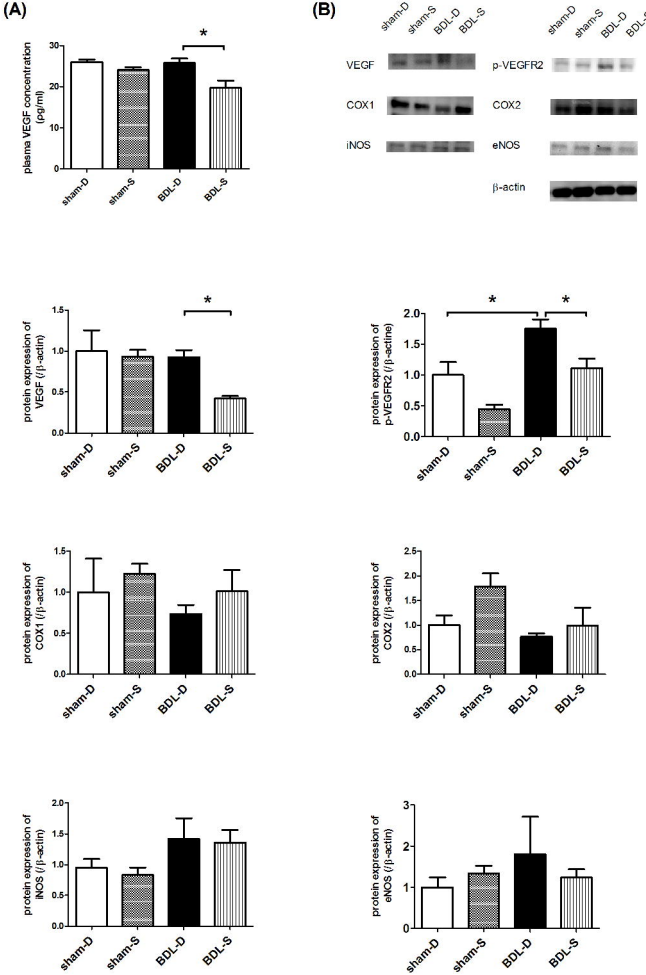
(A)
plasma VEGF concentration (pg/ml)
30
20
10
0
*
sham-D
sham-S
BDL-D
BDL-S
(B)
sham-D
sham-S
BDL-D
BDL-S
VEGF
COX1
iNOS
p-VEGFR2
COX2
eNOS
β-actin
protein expression of VEGF (/β-actin)
1.5
1.0
0.5
0.0
*
protein expression of p-VEGFR2 (/β-actine)
2.0
1.5
1.0
0.5
0.0
*
*
protein expression of COX1 (/β-actin)
1.5
1.0
0.5
0.0
protein expression of COX2 (/β-actin)
2.5
2.0
1.5
1.0
0.5
0.0
protein expression of iNOS (/β-actin)
2.0
1.5
1.0
0.5
0.0
protein expression of eNOS (/β-actin)
3
2
1
0

Figure 4

(A)

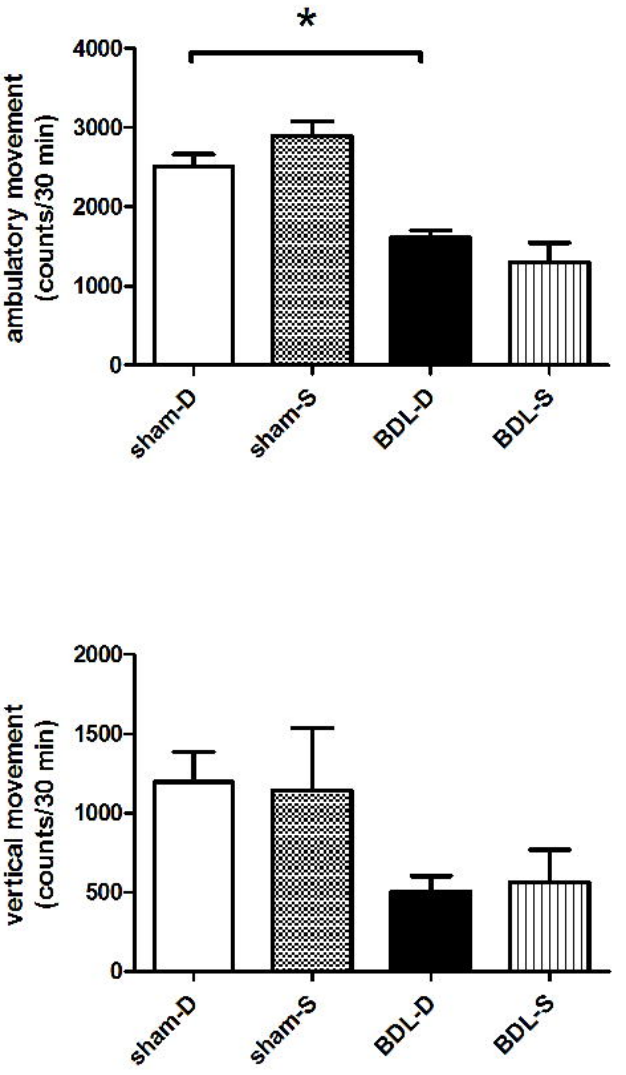
*
4000
3000
2000
1000
0
ambulatory movement
(counts/30 min)
sham-D
sham-S
BDL-D
BDL-S
2000
1500
1000
500
0
vertical movement
(counts/30 min)
sham-D
sham-S
BDL-D
BDL-S

(B)

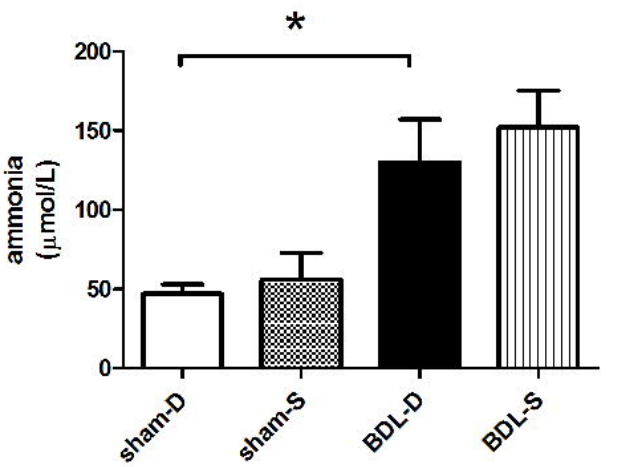
*
200
150
100
50
0
ammonia
(μmol/L)
sham-D
sham-S
BDL-D
BDL-S

Figure 5